EUV Lithography using Multi-Trigger Resist: performance improvements

C. Popescu[a], G. O'Callaghan[a], A. McClelland[a], C. Storey[a], J. Roth[b], E. Jackson[b], A.P.G. Robinson[a]

[a]*Irresistible Materials, Birmingham Research Park, Birmingham, UK*
[b]*Nano-C, 33 Southwest Park, Westwood, MA, USA.*
e-mail: a.p.g.robinson@bham.ac.uk

ABSTRACT

Novel resist materials will be required to support high-NA EUV with its decreased depth of focus and requirement for thinner films with higher photon absorbance. Irresistible Materials (IM) is developing novel resists based on the multi-trigger concept. In a multi-trigger resist (MTR) multiple elements must be simultaneously activated to enable a catalytic reaction. MTR shows wide dose and patterning flexibility with both formulation ratio and material library changes. MTR Gen1 introduced tunable absorbance as high as 18 μm^{-1}. MTR Gen2 introduces alternative choices of molecules to increase the monomer activation rate, optimize the ring opening polymerization reactions and improve the chain termination selectivity.

Here we present the lithographic performance at pitch 32 nm hexagonal pillars where 16nm diameter pillars were patterned using a 20 nm resist film at a dose of 43 mJ/cm^2 with an unbiased LCDU of 2.8 nm; or using a less sensitive formulation can be patterned at 74 mJ/cm^2 with an unbiased LCDU of 2.7 nm with fewer defects. We show staggered pillar results: pitch 36nm patterned at 51 mJ/cm^2 to obtain a pillar diameter of 17.5 nm with an unbiased LCDU of 2.2 nm. Additionally, p32 contacts of 16 nm diameter were patterned at 50 mJ/cm^2 with a biased LCDU of 3.77 nm. Using Gen 2.2 resist and a PEB of 85 °C, lines of 18.4 nm width at pitch 40 nm can be patterned using a 38 nm film thickness and 43 mJ/cm^2 dose.

Performance improvements such as reduced roughness and defectivity can also be shown to be affected by choices such as underlayer, stack and developer. We also show that the choice of organic underlayer is key to reducing touching pillar defects, and that the use of silicon rather than organic underlayer for pillar patterning further reduces the defectivity.

Keywords: EUV lithography, photoresist, molecular resist, multi-trigger resist, chemical amplification, crosslinking

1. INTRODUCTION

Intensive research for suitable resist materials to support the next generation EUV lithography, including the implementation of high-NA lithography, continues. It is commonly thought that development of new photoresist mechanisms is required as existing chemically amplified resists (CAR) will be unable to pattern the tightest pitches, and thus non-chemically amplified resists (non-CAR) are drawing more attention than ever before. Specifically, resists used for the current technology nodes are expected to reach a plateau in performance when it comes to simultaneously achieving the ultimate resolution, low line edge roughness, high sensitivity and low defectivity required in high-NA. [1–3] However, there remain many unknowns, which are slowing resist development and implementation, the most important being the mechanism by which the EUV photons interact within the photoresist film.

The energy of EUV photons is well above the ionization threshold of the resist materials, and thus photochemical approaches are not necessarily optimal in the EUV regime. The shift to secondary electron chemistry permits novel approaches to be developed. However, the mechanism of low energy electron interaction with resist molecules are not yet entirely clear and research to reveal the resist mechanism is ongoing. [4] Several approaches to explain photoacid generation have been proposed. These have included the ionization of the general resist matrix leading to electron recombination with photoacid generators producing photoacids either directly [5] or indirectly. [6] More recent work led by Brainard and co-workers, however, suggests an alternative mechanism based on internal excitations contributing to acid generation. [4,7]

Underlayer choice also plays an important role in the overall lithographic performance of resists. The events occurring at the interface between the photoresist and the silicon wafer are modulated by the chemical composition and the physical properties of the underlayer. This can be helpful or detrimental to the resolution and roughness in the features patterned, for instance by modulating the resist adhesion. The generation of secondary electrons in the underlayer may also be important. [8,9] Thermal properties of the underlayer may impact the speed of the resist chemistry. Furthermore, the underlayer choice also affects the metrology introducing contrast variations, depending on the underlayer used, in non-intuitive ways. [10] Finally, as industry moves towards the implementation of high-NA EUV to enable further improvements in resolution, it will become increasingly important to consider the overall thickness of the resist/underlayer stack. It has long been known that the achievable post development film thickness has needed to reduce, as pitch sizes decrease, to avoid pattern collapse, [11] and that this trend is accelerating. [12] However, film thicknesses will be further suppressed in high-NA, as the depth of focus of the tool is known to be severely constrained. [13] The metrology issues will also be exacerbated, and optimization of the underlayer/ photoresist stack will need to increase, whilst ever thinner photoresists will also introduce pattern transfer challenges. [14]

Irresistible Materials have developed the multi trigger resist (MTR) platform to address the on-going requirements of EUV lithography. The MTR material is a molecular resist, which utilizes ring-opening polymerization (ROP) and incorporates a unique self-quenching mechanism, known as the multi-trigger mechanism, directly in the chemical pathways, to improve performance. The intrinsic self-quenching mechanism in the MTR material, which has been described before [15–21] provides an advantage in acid diffusion mitigation and offers a benefit on achieving ultimate resolutions with low edge roughness. Transfer of lines and pillar patterns from MTR films using SiN as a hard mask and standard etch processes, even from thin films (26 nm post-coat; 24 nm post-development) has been demonstrated, [22] and p30 L/S have been successfully transferred from 18nm coated film thickness.

Initial results for MTR Generation 2 (Gen2) have been presented elsewhere. [23] Good lithographic performance was shown for P28 L/S with doses below 20 mJ/cm2 and p36 and p34 hexagonal pillars with doses below 30 mJ/cm^2. [22, 23] More recently we have explored three separate routes to significantly improve the Z-factor of the MTR system, either by increasing the activation rate of the monomer activation (Gen2.1); adjusting the relative reaction rates of the initiation and propagation rates of the ROP (Gen2.2); and via a more efficient multi-trigger quenching mechanism (Gen2.3). Additionally, the advantages gained by each approach are not correlated, and thus can be combined for further improvements of the MTR Z- factor (Gen2.4 and Gen 2.5). [24] Here we present new data showing the improvement shown by Gen 2.4, and also Gen 2.6, where all three improvement routes are combined.

2. EXPERIMENTAL

The resist samples were prepared by dissolving the individual components in ethyl lactate. The solutions are combined in various weight ratios and concentrations to give a range of formulations. The solutions undergo metal ion removal using 3M Zeta Plus filtration disks to reduce metals to levels appropriate for fab based processing.

The resist was spun onto a commercial organic underlayer, Brewer Scientific Optistack® AL412, unless stated. After spin-coating the resist the samples received a post application bake (PAB) of 80 °C for 1 minute, and the samples were exposed to EUV using an ASML NXE3400 scanner at imec. After exposure the samples received a post exposure bake of 65 °C unless stated and were developed in Fujifilm DP819A developer for 30 seconds using a dynamic system with no subsequent rinse. The patterning was observed using a Hitatchi CD-SEM (model 5000, 6300 or GT2000) and the LWR, LER, and LCDU values are biased values as measured inline unless otherwise stated. For selected wafers, MetroLER analysis using an appropriate number of images (25 for pillars, 50–100 for lines) at each dose was carried out to calculate unbiased LWR, LER and LCDU numbers, and also to calculate the defectivity (e.g. merged or missing pillars) for the sample.

3. RESULTS

3.1 Reducing defectivity in pillar patterning

The scope of this study was to reduce the defectivity of p32 hexagonal pillar patterns by means of formulation adjustment and underlayer choice. The defectivity of these pillars manifests as missing pillars in the underdosed region and as touching

pillars in the overdosed region. This evaluation was conducted by patterning the resist on a 5 nm thick bespoke organic underlayer. In figure 1 it can be observed that the sensitivity of the resist can be changed in such a way that at pillar diameters below 16.5 nm the change in LCDU is not significant. The 'fast' resist can pattern p32 hexagonal pillars with a diameter of 15.8 nm at a dose of 43 mJ/cm^2, whilst the 'slow' resist takes a dose of 74 mJ/cm^2 to pattern the same diameter. The unbiased LCDU values are very similar up to around 17 nm pillar diameter and are only 0.1nm different at 18 nm pillar diameter. The minimum LCDU is 2.3 nm for the 'slow' resist and 2.4 nm for the 'fast' resist. This metric by itself may suggest that the use of the faster resist is preferable. However, the defectivity shows that the slower resist has significantly fewer defects at all pillar diameters. This can be seen in the ADI pillar images as shown in figure 2. It should be noted that the 'slow' resist has a minimum ADI defect fraction of 4.0×10^{-5} for a pillar diameter of 15.30 nm, and that the defect type is merged pillars rather than missing pillars.

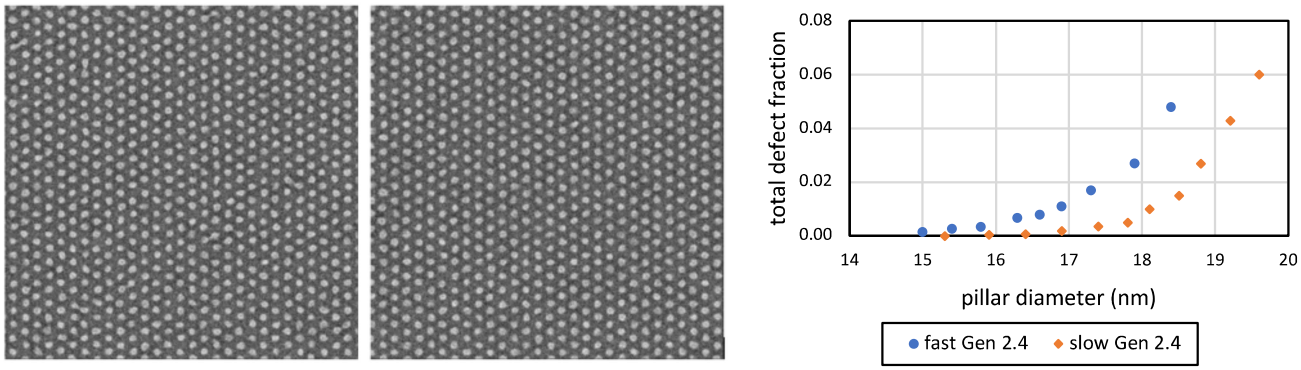

Figure 1: pillars patterned on the NXE3400 at p32 hex: (left) dose 43.1mJ/cm^2 'fast'; diameter 16.3 nm, unbiased LCDU 2.79nm; (middle) dose 74.1 mJ/cm^2 'slow'; diameter 16.4 nm, unbiased LCDU 2.71nm; (right) defect fraction

Most MTR pillar patterning has occurred using organic underlayers, with some preferred underlayers having material properties which enable patterning with lower roughness and defectivity. However, as shown previously, [22] MTR can be patterned directly onto SiN and used to transfer patterns.

In figure 2, we show MTR Gen 2.4 patterned directly on silicon compared to patterning on an organic underlayer. In this case, we see a 3 mJ/cm^2 reduction in dose to size and 0.2 nm reduction in LCDU when patterning on silicon. Patterning on silicon also results in fewer defects for pillars with diameters in the 14 nm to 17 nm region.

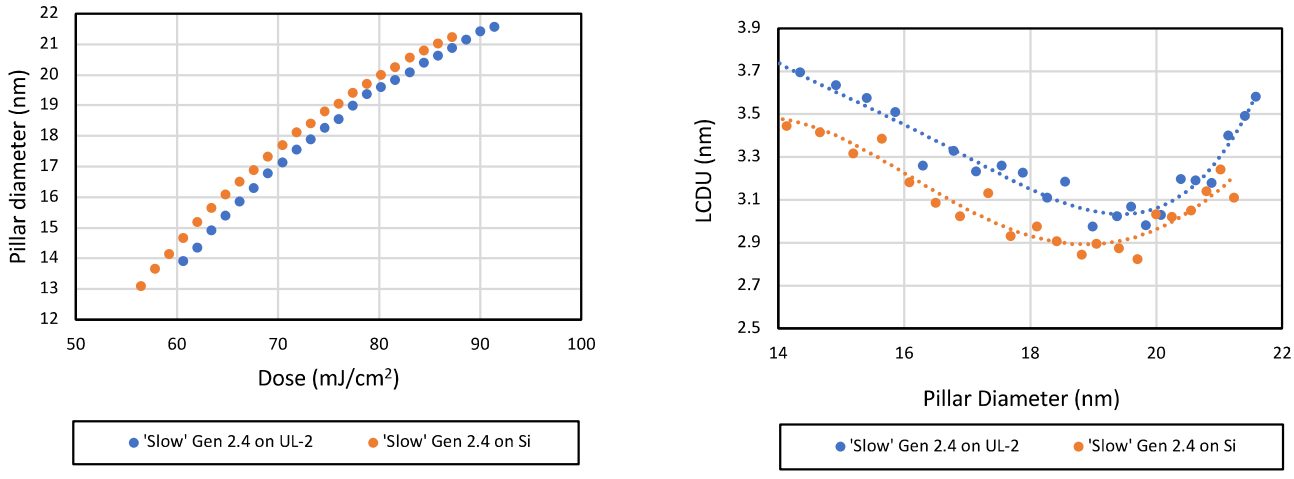

Figure 2: Pillar diameter versus dose, and biased LCDU versus diameter for p32 hex pillar patterning on organic underlayer and Si

MTR has also been used for p36 staggered pillar patterning for the first time. A 'fast' MTR Gen 2.4 variant was used at 3 different resist film thicknesses patterning directly onto silicon. The graph in figure 3 shows that increasing the film thickness decreases the measured biased LCDU in all regions up to 23 nm pillar diameter. Above this diameter, the increased number of touching pillars when using a thicker film shows itself in the higher LCDU value. Figure 3 also shows the staggered pillars at 18 nm diameter.

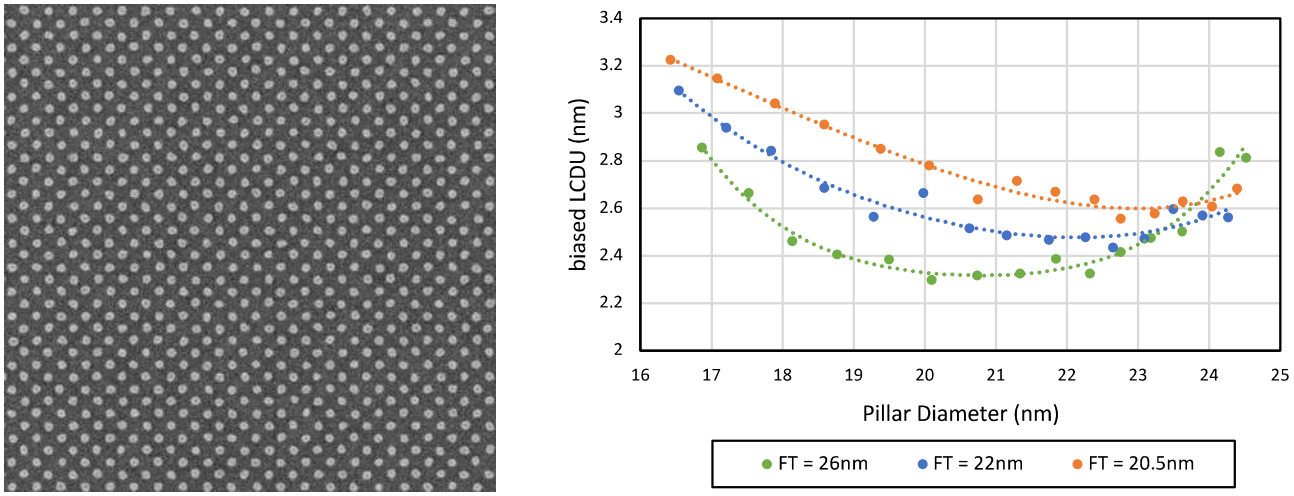

Figure 3: p36 staggered pillars patterned on NXE3400, dose 51.2 mJ/cm^2, diameter 17.49 nm, unbiased LCDU 2.19 nm; plot showing the measured LCDU (biased) as a function of pillar diameter

3.2. Optimization of MTR for dense lines and spaces

By varying the relative ratios of the MTR Gen 2.4 components it is possible to provide a resist with higher or lower sensitivity, depending on the application requirements. An experiment for dense line/spaces was carried out changing the formulation ratio to provide three different sensitivity resists. In addition to this, a Gen 2.1 resist with a dose midway between the Gen 2.4 'fast' and Gen 2.4 'mid' resist was patterned and compared. The spun film thickness for L/S was 20–22 nm and no PEB was applied. MetroLER analysis of the unbiased LER and defectivity has been plotted. As seen in figure 4, the dose to achieve 14 nm lines can be varied from 34 mJ/cm^2 to 58 mJ/cm^2.

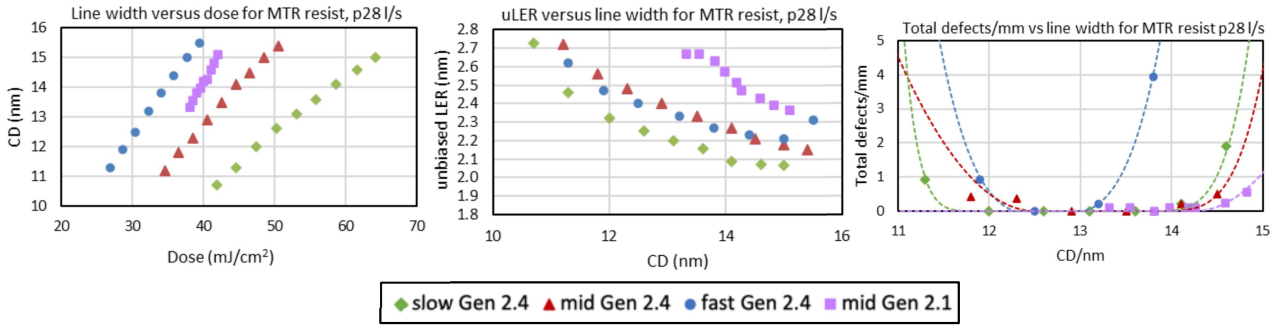

Figure 4: Line width as a function of dose (left), unbiased LER vs CD (middle) and defectivity vs CD (right) for p28 lines and spaces patterned on MTR Gen 2.1 and Gen 2.4. Analysed using MetroLER.

Gen 2.4 has significantly lower LER than the other samples, albeit at a higher dose and all Gen 2.4 resist variations have lower roughness than the Gen 2.1 resist. The results also suggest that the 'fast' Gen 2.4 resist gives similar roughness values to a resist ('mid' Gen 2.4) which requires 9 mJ/cm^2 more dose. However, less sensitive formulations show a wider failure free window for defects, as shown in figure 4. MetroLER analysis suggests that the failure free window for the 'slow' Gen 2.4 resist is at least from 12.0 nm to 13.6 nm (0 defects/mm) with <5 defects/mm between 11.3 nm and 14.6 nm linewidth (3.3 nm total window).

For double patterning applications, requiring low roughness, MTR can also be optimized to offer higher sensitivity or wider defect free window by customizing the formulation for the specified target. In figure 5 MTR Gen 2.2 was patterned using a dose of 42.7 mJ/cm^2 to achieve a CD of 18.4 nm at p40. Using MTR Gen 2.6 p36 was patterned using a dose of 29 mJ/cm^2 to obtain a CD of 15.59 nm. A variation of MTR Gen 2.6 can be used to pattern the same CD at a dose of 54 mJ/cm^2, which improved LWR and LER values by 0.3 nm.

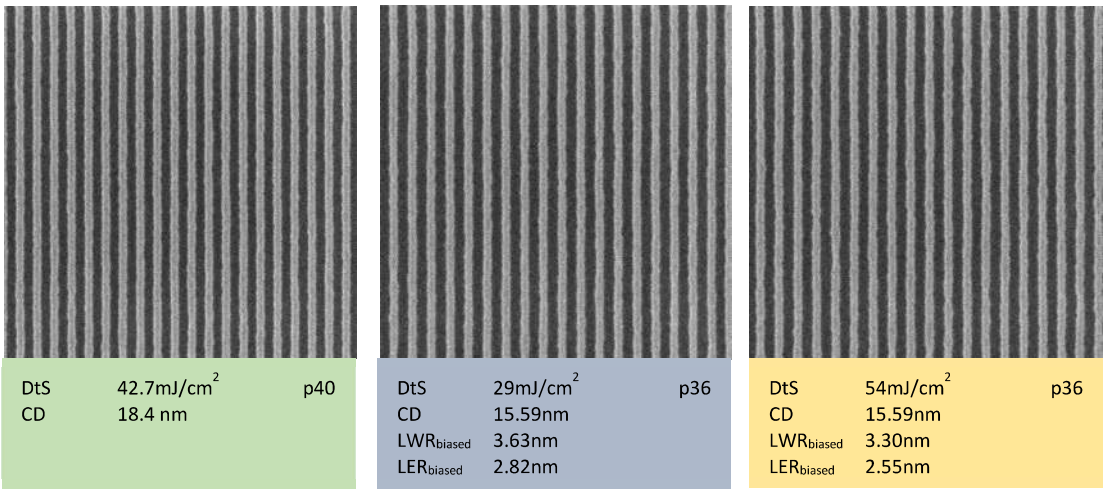

Figure 5: p40 using MTR Gen 2.2 resist (left), p36 using 'faster' MTR Gen 2.6 (middle), p36 using 'slower' MTR Gen 2.6 (right) line space patterned on NXE3400

3.3 Patterning Contact Holes using the MTR

The MTR material has recently been used to pattern contact holes using a bright field low-n reticle. These features are not commonly patterned using negative tone resists but the use of a bright field reticle together with the use of a negative tone resist such as the MTR material can bring advantages to the process. The dose required to pattern p32 hexagonal contact holes, see figure 6, was 39.5 mJ/cm^2 to achieve a diameter of 17.9 nm and the defect fraction was 0.

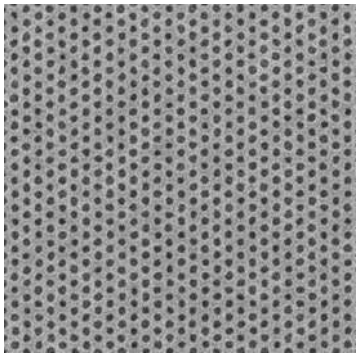

Figure 6: p32 hexagonal contact holes patterned on NXE3400 using a low n mask, dose 39.5 mJ/cm^2, diameter 17.9 nm, unbiased LCDU 2.56 nm, defect fraction = 0

4. CONCLUSIONS

MTR is a negative tone resist with an intrinsic dose dependent quenching mechanism, which can pattern high resolution patterns with EUV lithography. The lithographic performance of several MTR formulations was shown. By modifying the MTM molecule, crosslinker and PAG, both individually and in combination, we can optimize the reaction rates in the MTR mechanism. Different combinations have been designated Gen 2.1 to Gen 2.6 and here we show an LWR improvement in Gen 2.4 and 2.6 formulations. We presented the lithographic performance at pitch 28 nm dense line/space where 14.1 nm wide lines were patterned at 59 mJ/cm^2 with an unbiased LER of 2.09 nm using a Gen 2.4 resist. We showed hexagonal pillar results: pitch 32 nm patterned at 43 mJ/cm^2 to obtain a pillar diameter of 16 nm with an unbiased LCDU of 2.8 nm and additionally, p32 pillars of 16 nm diameter were patterned at 74 mJ/cm^2 with an unbiased LCDU of 2.7 nm. We also showed that staggered pillars at p36 can be patterned at 40 mJ/cm^2 for a biased pillar diameter of 18nm as well as p32 contact holes patterned with dose lower than 40 mJ/cm^2.

Performance improvements such as reduced roughness and defectivity can also be shown to be affected by choices such as underlayer and developer. We showed that using silicon, or in the future silicon-based layers, under the resist is a feasible alternative to an organic underlayer for pillars.

References

[1] Nagahara, S., Que Dinh, C., Yoshida, K., Shiraishi, G., Kondo, Y., Yoshihara, K., Nafus, K., Petersen, J.S., De Simone, D., Foubert, P., Vandenberghe, G., Stock, H-J, Meliorisz, B., "EUV resist chemical gradient enhancement by UV flood exposure for improvement in EUV resist resolution, process control, roughness, sensitivity, and stochastic defectivity," *Proc. SPIE*, **11326** (2020) 113260A.

[2] Shirotori, A., Hoshino, M., De Simone, D., Vandenberghe, G., Matsumoto, H., "A novel main chain scission type photoresists for EUV lithography", *Proc SPIE*, **11517** (2020) 115170D.

[3] Sharma, S.K., Kumar, R., Chauhan, M., Moinuddin, M.G., Peter, J., Ghosh, S., Pradeep, C.P., Gonsalves, K.E., "All-new nickel-based Metal Core Organic Cluster (MCOC) resist for N7+ node patterning," *Proc SPIE*, **11326** (2020) 1132604.

[4] Torok, J., Del Re, R., Herbol, H., Das, S., Bocharova, I., Paolucci, A., Ocola, L. E., Ventrice Jr., C., Lifshin E., Denbeaux, G., Brainard, R. L., "Secondary Electrons in EUV Lithography," *J Photopolym. Sci. Technol.*, **26** (2013) 625–634.

[5] Thackeray, J., Cameron, J., Jain, V., LaBeaume, P., Coley S., Ongayi O., Wagner M., Rachford A., Biafore J., "Progress in Resolution, Sensitivity and Critical Dimensional Uniformity of EUV Chemically amplified Resists," *Proc. SPIE*, **8682** (2013) 868213.

[6] Nakano, A., Kozawa, T., Okamoto, K., Tagawa, S., Kai, T., Shimokawa, T., "Acid Generation Mechanism of Poly(4-hydroxystyrene)-Based Chemically Amplified Resists for Post-Optical Lithography: Acid Yield and Deprotonation Behavior of Poly(4-hydroxystyrene) and Poly(4-methoxystyrene)," *Jpn. J. App. Phys.* **45**, (2006) 6866–6871.

[7] Narasimhan, A., Wisehart, L., Grzeskowiak, S., Ocola, L.E., Denbeaux, G., Brainard, R. L., "What we don't know about EUV exposure mechanisms," J Photopolym. Sci. Technol., **30** (2017) 113–120.

[8] Long, L.T., Neureuther, A., Walraff, G., Naulleau, P. "Resist Underlayer Simulations," In *IEUVI TWG April 2022*, 7, (2022), http://ieuvi.org/TWG/ Resist/IEUVI_Resist01.htm (Accessed 13/02/2023).

[9] Raley, A., Huli, L., Grzeskowiak, S., Lutker-Lee, K., Krawicz, A., Feurprier, Y., Liu, E., Kato, K., Nafus, K., Dauendorffer, A., Bae, N., LaRose, J., Metz, A., Hetzer, D., Honda, M., Nishizuka, T., Ko, A., Okada, S., Ido, Y., Onitsuka, T., Kawakami, S., Fujimoto, S., Shimura, S., Dinh, C.Q., Muramatsu, M., Biolsi, P., Mochiki, H. and Nagahara, S., "Outlook for high-NA EUV patterning: a holistic patterning approach to address upcoming challenges," *Proc SPIE*, **12056** (2022) 120560A.

[10] Severi, J., Lorusso, G.F., De Simone, D., Moussa, A., Saib, M., Duflou, R., De Gendta, S., "Chemically amplified resist CDSEM metrology exploration for high NA EUV lithography," *J Micro/Nanopattern. Mater. Metrol.*, **21** (2022) 021207.

[11] Goldfarb, D.L., Bruce, R.L., Bucchignano, J.J., Klaus, D.P., Guillorn, M.A. and Wu, C.J., "Pattern collapse mitigation strategies for EUV lithography," *Proc SPIE,* **8322** (2012) 832205.

[12] Noga, D.E., Lawson, R.A., Lee, C.T., Tolbert, L.M. and Henderson, C.L., "Understanding pattern collapse in high-resolution lithography: impact of feature width on critical stress." *Proc* SPIE, **7273** (2009) 727334.

[13] Burov, A., Pret, A.V. and Gronheid, R., "Depth of focus in high-NA EUV lithography: a simulation study." *Proc SPIE,* **12293** (2022) 122930V.

[14] Fallica, R., De Simone, D., Chen, S., Safdar, M. and Suh, H.S., "Scaling and readiness of underlayers for high-NA EUV lithography," *Proc* SPIE, **12292** (2022) 122920V.

[15] Vesters, Y., McClelland, A., Popescu, C., Dawson, G., Roth, J., Theis, W., de Simone, D., Vandenberghe, G., Robinson, A.P.G, "Multi-trigger resist patterning with ASML NXE3300 EUV scanner," *Proc. SPIE*, **10586** (2018) 1058308.

[16] Popescu, C., Kazazis, D., McClelland, A., Dawson, G., Roth, J., Theis, W., Ekinci, Y., Robinson, A.P.G., "High-resolution EUV lithography using a multi-trigger resist," *Proc SPIE*, **10583** (2018) 105831L.

[17] O'Callaghan, G., Popescu, C., McClelland, A., Kazazis, D., Roth, J., Theis, W., Ekinici, Y., Robinson, A.P. G., "Multi-trigger resist – Novel synthesis improvements for high resolution EUV lithography," *Proc SPIE*, **10960** (2019) 109600C.

[18] Montgomery, W., McClelland A., Ure D., Roth J., Robinson A., "Irresistible Materials multi-trigger resist: the journey towards high volume readiness," *Proc SPIE*, **10143** (2017) 1014328.

[19] Popescu, C., McClelland, A., Kazazis, D., Dawson, G., Roth, R., Ekinci, Y., Theis, W. and Robinson, A. P.G., "Multi-trigger resist for electron beam and extreme ultraviolet lithography," *Proc SPIE*, **10775** (2018) 1077502.

[20] Popescu C., O'Callaghan G., McClelland A., Roth J., Lada T., Robinson A.P.G., "Performance enhancements with high opacity multi-trigger resist," *Proc SPIE*, **11326** (2020) 1132611.

[21] Popescu, C., O'Callaghan, G., McClelland, A., Roth, J., Lada, T., Kudo, T., Dammel, R., Moinpour, M., Cao, Y., Robinson, A. P. G., "Progress in the multi-trigger resist," *Proc SPIE*, **11612** (2021) 116120K.

[22] Popescu, C., O'Callaghan, G., McClelland, A., Roth, J., Jackson, E., Robinson, A. P. G., "Component optimization in the multi-trigger resist," *Proc SPIE*, **12055** (2022) 120550G.

[23] Popescu, C., O'Callaghan, G., McClelland, A., Storey, C., Roth, J., Jackson, E. and Robinson, A.P.G., " Recent accomplishments in EUV lithography patterning for multi-trigger resist," *Proc SPIE*, **12292** (2022) 122920E.

[24] Popescu, C., O'Callaghan, G., McClelland, A., Storey, C., Roth, J., Jackson, E. and Robinson, A.P.G., "EUV lithography patterning using multi-trigger resist," *Proc SPIE*, **12498** (2023) 1249812.

[25] Lawson, R.A., Frommhold, A., Yang, D.X., Robinson, A.P.G, "Negative-tone organic molecular resists," In *Frontiers of Nanoscience*: *Materials and Processes for Next Generation Lithography*, **Vol. 11**, Robinson A.P.G. and Lawson R.A. eds., (Oxford: Elsevier, 2016). pp. 223-317.